Experimental and Numerical Analysis of S-CO_2 Critical Flow for SFR Recovery System Design

Min Seok Kim, Hwa-Young Jung, Yoonhan Ahn, Jekyoung Lee, Jeong Ik Lee*
Department of Nuclear and Quantum Engineering, Korea Advanced Institute of Science and Technology
**Corresponding author: jeongiklee@kaist.ac.kr*

1. Introduction

Current Sodium-cooled Fast Reactor (SFR) design may face difficulty in public acceptance due to the potential risk from sodium-water reaction (SWR) when the current conventional steam Rankine cycle is utilized as a power conversion system. In order to eliminate SWR, a concept of coupling the Supercritical CO_2 (S-CO_2) cycle with SFR has been proposed. It is known that for a closed system controlling the inventory is important for stable operation and achieving high efficiency. Since the S-CO_2 power cycle is a highly pressurized system, certain amount of leakage flow is inevitable in the rotating turbo-machinery via seals. The parasitic loss caused by the leakage flow should be minimized since this directly influences the cycle efficiency. Thus, a simple model for estimating the critical flow in a turbo-machinery seal is essential to predict the leakage flow rate and calculate the required total mass of working fluid in a S-CO_2 power system to minimize the parasitic loss. This paper presents both numerical and experimental studies of the critical flow of S-CO_2 while special attention is given to the turbo-machinery seal design. A computational critical flow model is described first. The experiments were conducted to validate the critical flow model. Various conditions have been tested to study the flow characteristic and provide validation data for the model. The comparison of numerical and experimental results of S-CO_2 critical flow will be presented.

2. Numerical Study

2.1 Model Development

As mentioned in the introduction, certain amount of leakage flow from the system is inevitable in the rotating turbo-machinery since the S-CO_2 power cycle is a highly pressurized system. CO_2 flow in a turbo-machinery through seal will be mostly choked flow due to a large pressure difference between the rotor cavity and lower pressure station. However, only limited information is available for estimating CO_2 critical flow expanding from supercritical state to gas state [1], [2].

In this work, the final goal is to simulate transient response of the high pressure side and low pressure side during the CO_2 leak process realistically. In a real operation, the CO_2 flow is a compressible flow, which can be choked depending on the pressure difference. The mass flow rate is determined from the seal size and the mass flux determined from the flow resistance and pressure drop. To model the CO_2 leak flow mechanism realistically, several complex factors should be considered and a few assumptions are necessary for model simplification. Thus, in this study, simplified flow model was developed as the first step toward the complete model to predict the CO_2 leak flow process. The simplified flow model assumes isentropic flow and the model was developed with several assumptions. Assumptions for the isentropic flow model are as follows:

1. CO_2 in operating condition behaves like ideal gas. (Compressibility factor ≈ 1)
2. CO_2 is stagnant in the CO_2 tanks.
3. Whether the flow is choked or not depends on the conditions of high pressure CO_2 tank and the low pressure CO_2 tank.
4. The under-expansion of CO_2 at the nozzle exit is neglected.

It should be checked whether the flow is choked or while pressure is varying over time. If the flow is choked, the maximum flow velocity of CO_2 has been reached, and the amount of leaked CO_2 will rapidly increase with time.

2.2 Numerical Model

To simplify the expected CO_2 leak flow in a turbo-machinery, a simplified model for CO_2 leak flow simulation was constructed as shown in Fig. 1.

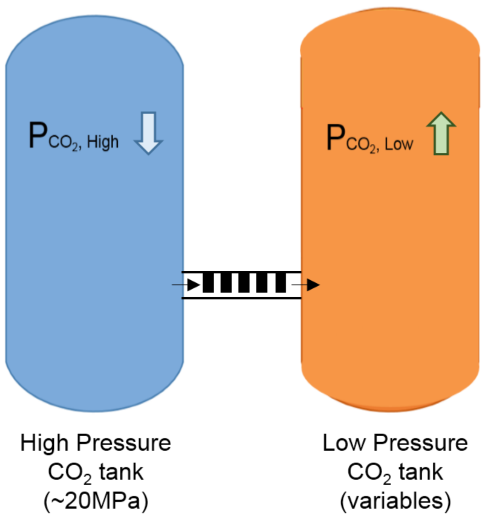

Fig. 1. Conceptual diagram of the simplified model for a numerical analysis

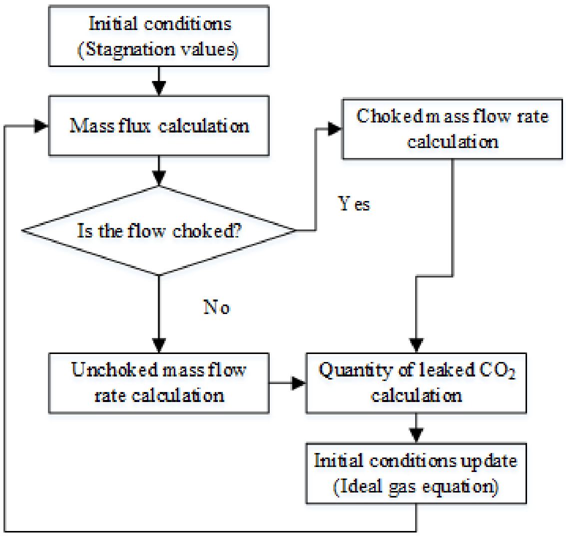

Fig. 2. Flow chart of CO_2 critical flow model

The calculation of CO_2 critical flow model for evaluating the leak rate of CO_2 in a turbo-machinery is referred from the CO_2 leak model of Na-CO_2 heat exchanger in the S-CO_2 power cycle [3]. It was assumed that CO_2 flows through a nozzle from a high pressure CO_2 tank to a low pressure CO_2 tank, and the nozzle diameter plays the same role as the seal size.

For an isentropic flow, the frictional pressure loss and heat transfer are neglected thus the flow state can be easily calculated with the following governing equations (i.e. continuity equation, critical-pressure ratio equation, Mach number equation with pressure ratio, and mass flux equation from continuity equation):

$$G = \rho V_{elovity} = constant \tag{1}$$

$$\frac{P_0}{P_{critical}} = \left(1 + \frac{\gamma - 1}{2}\right)^{\gamma/(\gamma-1)} \tag{2}$$

$$M = \sqrt{\frac{2}{\gamma - 1}\left[\left(\frac{P_0}{P}\right)^{(\gamma-1)/\gamma} - 1\right]} \tag{3}$$

$$G = \frac{P_0}{\sqrt{RT_0}}\sqrt{\gamma}M\left(1 + \frac{\gamma - 1}{2}M^2\right)^{-\frac{\gamma+1}{2(\gamma-1)}} \tag{4}$$

$$G_{max} = \frac{P_0}{\sqrt{RT_0}}\sqrt{\gamma}\left(\frac{\gamma + 1}{2}\right)^{-\frac{\gamma+1}{2(\gamma-1)}} \tag{5}$$

Based on the above governing equations, the critical pressure obtained from Eq. (2) is compared to the low pressure side at every time step. The choked condition is then checked. If the flow is not choked, Mach number is calculated from Eq. (3) and it is applied to Eq. (4). On the other hand, Eq. (5) with Mach number of unity is used to calculate the choked mass flux.

To simplify the model, it was assumed that temperature and pressure of CO_2 at the seal exit are at equilibrium with CO_2 in the low pressure tank.

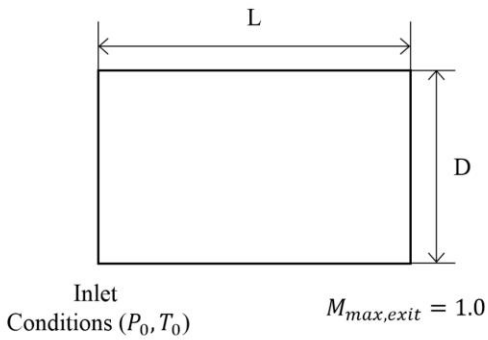

Fig. 3. Configuration of nozzle for CO_2 critical flow model

This assumption actually neglects expansion process of CO_2 at the nozzle exit although the CO_2 pressure at the exit is higher than that of CO_2 in the low pressure tank when the flow is choked. Fig. 2 shows a flowchart of the CO_2 critical flow model. By updating the changed pressure and temperature of CO_2 in each time step, mass flux is calculated until both tanks reach equilibrium. A configuration of the nozzle is shown in Fig. 3. Based on the algorithm of the CO_2 critical flow model, the sensitivity study of the transient response during the leak process was performed while varying nozzle diameter and initial conditions (temperature and pressure).

3. Experimental Study

3.1 Experiments

3.1.1 Designed Experimental Facility

To validate the CO_2 critical flow model with experiments, a critical flow test facility was designed. Fig. 4 shows the designed experimental facility for the CO_2 leak test and the design specifications are shown in Table I. For an accurate measurement, total nine thermocouples, and seven pressure gauges were installed on the critical flow facility.

Fig. 4. Designed experimental facility for the CO_2 leak test

Table I: Design specifications for experimental facility

	Design Parameters	
High/Low-pressure tank	Pressure (MPa)	22
	Temperature (℃)	150
	Volume (L)	47 (I.D.:200 mm, H: 1600mm)
Pipe connecting two tanks	Internal diameter (mm)	57
	Length (mm)	1090
Heater (Jacket-type)	Electric capacity (kW)	5
Valve type	Ball valve	

Three thermocouples and two pressure gauges were installed on the high pressure tank (left) and the low pressure tank (right), respectively. Moreover, one thermocouple and one pressure gauge was installed between high pressure tank and a ball valve.

To control the initial temperature of the high pressure tank, heater covers external of the high pressure tank. By injecting the CO_2 gas through a booster pump, pressure of the high pressure tank can be controlled. Opening the ball valve without delay is important for comparison of the model and the data as the CO_2 critical flow model calculates the mass flux without considering the valve opening time. Therefore, the ball valve is automatically opened and driven by hydraulic pressure (10 bar) from an air compressor to open the ball valve quickly. Diameter and length of the designed nozzle can be changed.

3.1.2 Experiment Conditions

Initial conditions of the low pressure tank was maintained to be the same with the ambient condition (about 15℃, 0.101MPa) to maximize the pressure difference and have long depressurization time for stable measurement of the CO_2 critical flow. The initial pressure of the high pressure tank was changed from 10MPa to 20MPa since the S-CO_2 power cycle is a highly pressurized system. The maximum pressure of designed S-CO_2 power cycle for a SFR application is usually 20MPa. The initial temperature of the high pressure tank was changed from 100℃ to 150℃ because the main compressor and the re-compressor outlet temperatures (i.e. where the seals are) are around the 100℃ and 150℃, respectively.

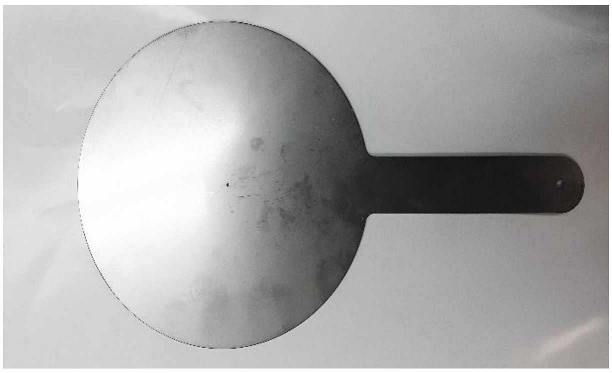

Fig. 5. The specific design of the nozzle

Table II: Experimental conditions

Parameters	Conditions	
Nozzle diameter (mm)	1.5	
Length (mm)	5.0	
Pressure (MPa)	High pressure tank	10~20
	Low pressure tank	0.101
Temperature (℃)	High pressure tank	100~150
	Low pressure tank	15

Table III: Summary of experimental cases

		1	2	3
High pressure tank	P (MPa)	10.04	13.43	20.16
	T (℃)	103.3	161.5	151.2
Low pressure tank	P (MPa)	0.101	0.101	0.101
	T (℃)	14.5	15.6	14.1

The specific design of the nozzle is shown in Fig. 5, experimental parameters and preset values are summarized in Table II, and three experimental cases are summarized in Table III.

3.1.3 Experiment Results

To compare the experimental results with the CO_2 critical flow model, three legends are first explained for the clarification. Legend 1 results are the experimental results obtained from the experimentally measured pressures and temperatures directly. Legend 2 and Legend 3 are the numerically obtained results from the CO_2 critical flow model. Legend 2 used the experimentally measured pressures and temperatures of each CO_2 tank as the boundary conditions to calculate the mass flux. Legend 3 used the initially measured pressure and temperature of each CO_2 tank and calculated the pressure and temperature changes of each tank from the calculated mass flux for every time step. In short, pressure and temperature of both tanks were simulated from the measured initial conditions.

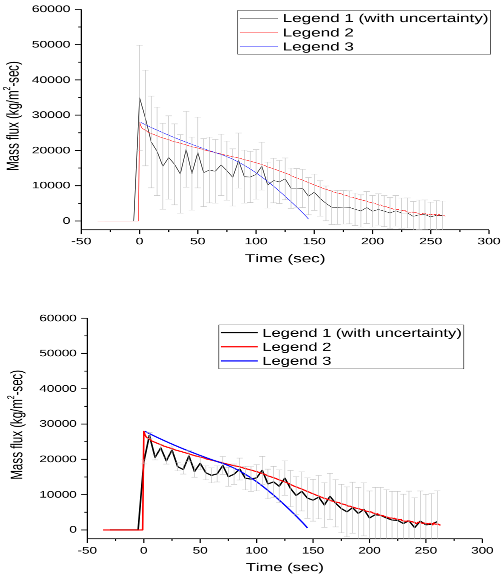

Fig. 6. Mass flux result of experiment and model using condition of HP tank (upper), and LP tank (lower) [Case 1]

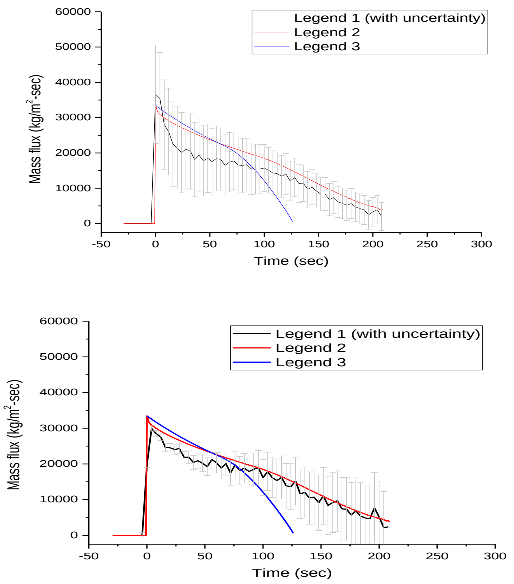

Fig. 7. Mass flux result of experiment and model using condition of HP tank (upper), and LP tank (lower) [Case 2]

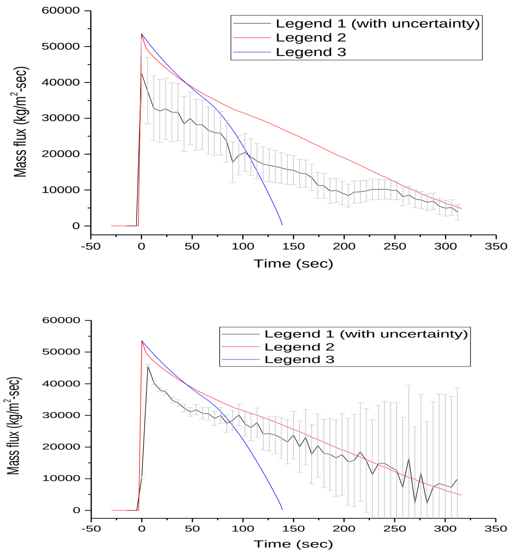

Fig. 8. Mass flux result of experiment and model using condition of HP tank (upper), and LP tank (lower) [Case 3]

From Fig. 6 to Fig. 8, comparisons of mass flux between the CO_2 critical flow experimental results and the CO_2 critical flow model for three cases are shown. In the first case, which the initial conditions of the high-pressure tank are 10.01 MPa and 103.3 ℃, the mass flux of the CO_2 leak experimental results and the CO_2 critical flow model agree with each other quite well. It is indicated that the developed CO_2 critical flow model can simulate the real CO_2 leak flow. However, the temperature difference between the experimental result (Legend 1) and the calculated tank temperature (Legend 3) is relatively big. This difference is found in not only for case 1 but also for cases 2 and 3. It seems to be due to thermal inertia and insufficient insulation of the CO_2 critical flow facility. Heat loss from the experimental facility seems to be significant since only the high-pressure tank was insulated and other parts including connecting pipes and the low-pressure tank did not have insulation. The second reason is the thermal inertia of the heater which surrounds the high-pressure tank and the tank itself. After reaching the target initial conditions of the high-pressure tank, the heater was turned off during the experiment. The CO_2 critical flow model in Legend 3 does not consider heat transfer effect from CO_2 to the tank and tanks have thermal inertia. Consequently, these effects induced the temperature difference between the experimental and numerical results. In the second and third cases, the mass flux calculated from the measured values has similar trend with the result of CO_2 critical flow model as shown in Figs. 7 and 8. All the presented mass flux results in the figures include the uncertainty bar.

4. Conclusions

An experiment of CO_2 critical flow was performed to verify the real CO_2 flow behavior and validate the CO_2 critical flow model with experimental results. The mass flux calculated from the measured values has similar trend with the results of the CO_2 critical flow model in all cases. It is identified that the developed isentropic critical flow model can estimate the behavior of the CO_2 critical flow in a S-CO_2 turbo-machinery.

To simulate the CO_2 leak flow in a turbo-machinery with higher accuracy in the future, the real gas effect and friction factor will be considered for the CO_2 critical flow model. Moreover, experimentally obtained temperature data were somewhat different from the numerically obtained temperature due to the insufficient insulation and large thermal inertia of the CO_2 critical flow facility. Insulation in connecting pipes and the low-pressure tank will be added and additional tests will be conducted.

Actually, the developed CO_2 critical flow model does not correctly reflect a labyrinth seal geometry effect. The real labyrinth seal has multiple tooth to further minimize the leak. Therefore, to upgrade the numerical model by applying the labyrinth seal geometry effect and conducting an experiment of a real labyrinth seal geometry nozzle will be performed in the near future.

REFERENCES

[1] Hylla, E., Schildhauer, M., Bussow, R., Metz, K., Klawes, R., 2015, “Investigations on Transonic Flow of Super-critical CO_2 Through Carbon Ring Seals”. ASME Turbo Expo (2015).
[2] G.P. Mignot, M.H. Anderson, M.L. Corradini, Measurement of supercritical CO_2 critical flow: effects of L/D and surface roughness, Nucl. Eng. Des. 239 (2009) 949–955.
[3] Hwa-Young Jung. Preliminary Safety Studies of Sodium-CO_2 Heat Exchanger in SFR coupled with S-CO_2 Brayton Cycle. Thesis, KAIST (2015).